

# Substrate limited electron dynamics in graphene

S. Fratini<sup>1,2</sup>, F. Guinea<sup>2</sup>

<sup>1</sup> *Institut Néel - CNRS & Université Joseph Fourier, BP 166, F-38042 Grenoble Cedex 9, France*

<sup>2</sup> *Instituto de Ciencia de Materiales de Madrid. CSIC, Sor Juana Inés de la Cruz 3, E-28049 Madrid, Spain*

(Dated: November 14, 2018)

We study the effects of polarizable substrates such as SiO<sub>2</sub> and SiC on the carrier dynamics in graphene. We find that the quasiparticle spectrum acquires a finite broadening due to the long-range interaction with the polar modes at the interface between graphene and the substrate. This mechanism results in a density dependent electrical resistivity, that exhibits a sharp increase around room temperature, where it can become the dominant limiting factor of electron transport. The effects are weaker in doped bilayer graphene, due to the more conventional parabolic band dispersion.

PACS numbers: 71.20.Tx 72.10.Di 73.63.-b

*Introduction.* Remote phonon scattering is a known limiting factor of the electron mobility in two-dimensional artificial structures of technological interest, such as Si MOSFETs [1, 2, 3, 4]. Due to the polar nature of the gate dielectrics used in such devices, the carriers in the conducting channel couple electrostatically to the long-range polarization field created at the conductor/dielectric interface. The interaction occurs primarily with optical phonon modes of high frequency (50 – 200 meV), which do not affect transport at low temperatures. However, it results in a sizable degradation of the mobility at room temperature (i.e. the temperature of device operation), and becomes the dominant scattering mechanism in devices with high- $\kappa$  gate dielectrics.

The interaction with the phonons of the gate dielectric has been recently investigated in another class of electronic devices, where the Si inversion layer is replaced by a crystalline organic semiconductor [5, 6]. In organic FETs, due to the narrow-band nature of the active material (typical bandwidths are less than 0.5 eV), the energy scale associated to the remote phonon interaction can become comparable with the bandwidth, resulting in carrier self-localization. In this case the effect is more dramatic than in Si MOSFETs: the mobility is not only strongly reduced by the interactions, but it also acquires an exponentially activated temperature dependence, due to the hopping motion of the localized carriers.

Graphene –an atomically thin sheet of carbon atoms– is another system where the long-range coupling to the polar modes of the substrate can have a sizable influence on carrier dynamics. Compared to the two-dimensional electron gas formed in Si inversion layers, the effect here is enhanced due to the poor screening properties of the quasiparticles close to the nodal points, which behave as Dirac fermions. Although most experimental studies of transport in graphene up to now have focused on the low temperature regime [7, 8], its possible use as a material basis for future electronic devices calls for a deeper understanding of the room temperature behavior [9, 10, 11, 12, 13].

In this work we calculate the effects of remote phonon scattering on the dynamics of electrons in graphene [14]. Unlike other scattering mechanisms such as disorder [15, 16, 17, 18, 19], or acoustic phonon scattering [20], all the microscopic parameters of the remote electron-phonon interaction are known *a priori* from independent measurements, so that in principle its effects can be estimated quantitatively. We show that in epitaxial graphene grown on SiC, the polar phonon scattering has only a weak effect on the electron mobility, due to the weak polarizability of the substrate and the relatively high phonon frequencies associated to the hard Si-C bonds. The effect is much larger at graphene/SiO<sub>2</sub> interfaces where, at room temperature and at the typical densities  $n \gtrsim 10^{12} \text{cm}^{-2}$  attained in current experiments, it gives rise to resistivities of the order of 100 $\Omega$ . This suggests that, as in traditional Si based electronic devices, remote scattering with the substrate phonons can indeed constitute an important limiting factor of the mobility in future graphene devices.

*The model.* The polar phonons of the substrate induce an electrostatic potential which couples to the electron charge. This potential is smooth over lengths comparable to the lattice constant, due to the finite distance between the substrate and the graphene layer (see below), which allows us to neglect intervalley scattering. In this case the electron-phonon interaction term is given by  $H_I = \sum_q M_q \rho_q (b_q + b_{-q}^\dagger)$ , where  $\rho_q$  is the electron density operator and the operators  $b_q^\dagger, b_q$  describe the phonon displacements. The interaction matrix element can be written as  $M_q^2 = g e^{-2qz}/(qa)$  [1, 2, 3, 21], where  $z$  is the distance between the graphene layer and the substrate and  $a = 1.42 \text{Å}$  is the lattice spacing. Neglecting the dielectric response of the atomically thin graphene layer, the dimensionless coupling parameter  $g$  is given by

$$g = 2\pi\beta \frac{\hbar\omega_s}{\hbar v_F/a} \frac{e^2}{\hbar v_F}. \quad (1)$$

Here  $\beta = (\epsilon_s - \epsilon_\infty)/(\epsilon_s + 1)/(\epsilon_\infty + 1)$  is a combination of the known dielectric constants of the substrate,  $v_F =$

$10^6$  cm/s the Fermi velocity and  $\omega_s$  the frequency of the interface phonon mode under consideration. We consider separately the case of epitaxial graphene grown on SiC, and that of graphene flakes deposited on SiO<sub>2</sub> substrates.

In 6H-SiC there is a single surface phonon mode at  $\omega_s = 116$ meV [22]. The dielectric constants of the bulk material are  $\epsilon_s = 9.7$ ,  $\epsilon_\infty = 6.5$ , which yields  $\beta = 0.040$  and  $g = 1.7 \cdot 10^{-2}$ . In the case where several surface modes are present, as in SiO<sub>2</sub>, each mode will couple through a partial factor  $\beta_i$  weighted by its oscillator strength (the sum of all  $\beta_i$ 's still given by  $\beta$  defined above). For example, in crystalline SiO<sub>2</sub> ( $\epsilon_s = 3.9$ ,  $\epsilon_\infty = 2.4$ ), there are two dominant surface modes at  $\omega_{s1} = 59$  meV and  $\omega_{s2} = 155$  meV, with  $\beta_1 = 0.025$  and  $\beta_2 = 0.062$  respectively ( $\beta = 0.087$ ) [3], corresponding to  $g_1 = 5.4 \cdot 10^{-3}$  and  $g_2 = 3.5 \cdot 10^{-2}$ . These values are enhanced by roughly 50% in common SiO<sub>2</sub> glass, where  $\epsilon_\infty = 2.1$ . For completeness, we also give the values for the high- $\kappa$  dielectric HfO<sub>2</sub> that has been used in recent experiments on locally gated graphene [23]:  $\epsilon_s = 22$ ,  $\epsilon_\infty = 5$ ,  $\beta = 0.12$  and  $\omega_s \simeq 94$ meV, so that  $g = 4.2 \cdot 10^{-2}$ .

*Scattering rate.* The quasiparticle scattering rate arising from the remote electron-phonon interaction described above can be calculated as

$$\Gamma(\omega) = \frac{\pi}{2} \sum_{\mathbf{q}} A_{\mathbf{p},\mathbf{q}} M_q^2 \left\{ \delta(\epsilon_{\mathbf{p}+\mathbf{q}} - |\omega + \omega_s|) [n_B + n_F^+] + \delta(\epsilon_{\mathbf{p}+\mathbf{q}} - |\omega - \omega_s|) [n_B + 1 - n_F^-] \right\}, \quad (2)$$

where the band dispersion is  $\omega = \pm \epsilon_{\mathbf{p}} = \pm v_F p$ ,  $n_B$  is the Bose distribution for phonons of energy  $\omega_s$  and  $n_F^+, n_F^-$  are the Fermi functions for electrons at  $\omega \pm \omega_s$ . The factor  $A_{\mathbf{p},\mathbf{q}} = [1 + s \cos(\phi_{\mathbf{p}+\mathbf{q}} - \phi_{\mathbf{p}})]/2$  is the spinor overlap for intraband ( $s = 1$ ) and interband ( $s = -1$ ) scattering respectively, where  $\phi_{\mathbf{p}}$  defines the direction of  $\mathbf{p}$ . To a first approximation, dynamic screening from the conduction electrons can be accounted for by replacing  $1/q \rightarrow 1/(q + q_s)$  in the interaction matrix element  $M_q^2$ , where  $q_s = 4e^2 k_F / \hbar v_F$  is the Thomas-Fermi screening length [24]. We set the graphene/substrate distance to the typical value  $z = 4\text{\AA}$ . Eq. (2) can be directly generalized to bilayer graphene, by considering a parabolic band dispersion  $\epsilon_p = v_F^2 p^2 / t_\perp$ , with  $t_\perp \sim 0.35$ eV the interlayer hopping parameter. In that case the screening wavevector becomes independent of band filling,  $q_s = 4t_\perp / \hbar v_F$ , and the spinor overlap changes to  $[1 + s \cos 2(\phi_{\mathbf{p}+\mathbf{q}} - \phi_{\mathbf{p}})]/2$ . We also take a slightly larger separation  $z \simeq 6\text{\AA}$ , corresponding to the average distance of the bilayer to the interface, although in principle the electron-phonon coupling differentiates between the two graphene sheets.

In Fig.1 we show plots of the scattering rate  $\Gamma$  corresponding to single-layer and bilayer graphene on the two different substrates SiC and SiO<sub>2</sub>, for both undoped ( $E_F = 0$ ) and heavily doped ( $E_F = 0.6$ eV) graphene. In all cases the scattering rate is suppressed in a window  $\pm \omega_s$  around the Fermi energy (it actually vanishes

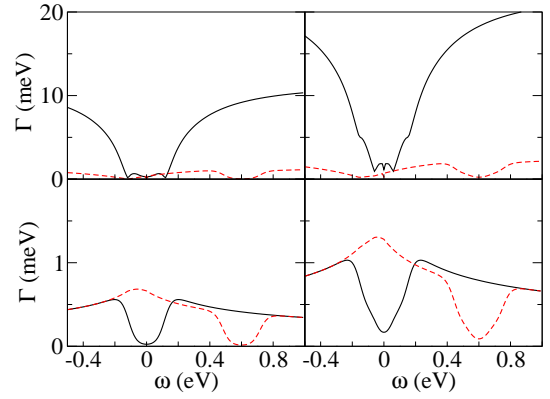


FIG. 1: Quasiparticle's scattering rate due to remote phonon interaction as function of energy for: single-layer (top) and bilayer (bottom) graphene, with the parameters appropriate to an SiC (left) and a SiO<sub>2</sub> (right) substrate respectively. The full and dotted lines correspond respectively to undoped,  $E_F = 0$ , and heavily doped,  $E_F = 0.6$ eV cases. Notice the different axis scale in single-layer (top) and bilayer graphene (bottom).

at  $T = 0$ , because in that case phonon exchange is forbidden in all this range). The absolute value of  $\Gamma$  at the chemical potential, that will enter in the calculation of the d.c. conductivity, is proportional to both the coupling strength  $g$  and the phonon thermal population, i.e.  $\Gamma \propto g e^{-\omega_s/T}$ . Note that the anomalously large scattering rates obtained for undoped single-layer graphene (full lines in the upper panels of Fig. 1) compared to all the other cases are related to the poor screening properties of Dirac electrons close to the neutrality point.

The present results for the quasiparticle lifetimes from remote phonon scattering can be compared with analogous estimates for the interaction with the intrinsic in-plane vibrations of the graphene sheet [25]. The effect of the substrate appears to be slightly weaker than the intrinsic electron-phonon scattering in the case of epitaxial graphene grown on SiC, while the two mechanisms are of comparable magnitude at graphene/SiO<sub>2</sub> interfaces. Nevertheless, we will show below that due to the smaller oscillation frequencies involved, remote phonons have a much stronger influence on electronic transport than the intrinsic phonons of graphene.

*Conductivity.* We calculate the electrical conductivity through the Boltzmann equation. Taking into account spin and valley degeneracy, the d.c. conductivity of single-layer graphene can be expressed as:

$$\sigma = \frac{e^2}{h} \int d\omega |\omega| \Gamma_{tr}^{-1}(\omega) \left( -\frac{dn_F}{d\omega} \right). \quad (3)$$

Here  $\Gamma_{tr}(\omega)$  is the transport scattering rate, defined as in Eq.(2), with the additional angular factor  $[1 - s \cos(\phi_{\mathbf{p}+\mathbf{q}} - \phi_{\mathbf{p}})]$  in the integrand which favors large angle scattering events [26]. Note that this approximation is strictly valid only in the elastic limit  $\omega_0 \rightarrow 0$  (where

$\Gamma_{tr} \approx \Gamma/2$ ) while it slightly underestimates the scattering rate in the inelastic regime  $\omega \lesssim \omega_0$ . In the case of bilayer graphene, the integral in Eq. (3) has an additional factor  $2\omega/t_{\perp}$  arising from the parabolic band dispersion.

We now present results for graphene on  $\text{SiO}_2$  substrates, where most experimental transport measurements have been performed (the predicted effect at room temperature is one order of magnitude smaller in the case of SiC). From Eq. (3), since the derivative of the Fermi function selects contributions close to the Fermi energy, we see that the conductivity is inversely proportional to the scattering rate at  $\omega \simeq E_F$ , which in turn scales as  $ge^{-\omega_s/T}$  (see above). Since the coupling constant  $g$  in Eq. (1) is directly proportional to the phonon frequency  $\omega_s$ , we see that the scattering rate at a given temperature  $T$  is a non-monotonic function of the phonon frequency: it is maximum at  $\omega_s = T$ , and decreases exponentially for larger phonon frequencies. As a result, the phonons that mostly affect transport will be the ones with the lowest frequencies (closest to  $T$ ). In particular, in the case of a  $\text{SiO}_2$  substrate, the dominant phonon is the one at  $\omega_{s1} = 59\text{meV}$ , even though it has a weaker coupling strength (due to the exponential temperature dependence, scattering from the phonon at  $\omega_{s2} = 155\text{meV}$  is mostly inactive at room temperature). For the same reason, in-plane optical phonons whose characteristic energy scale is  $\sim 200\text{meV}$  should give a negligible contribution to the resistivity at room temperature.

*Results.* In Fig. 2a we show the result of  $\rho$  vs  $T$  at  $E_F = 100\text{meV}$  (corresponding to a density  $n = 0.7 \cdot 10^{12}\text{cm}^{-2}$ ) taking a finite distance  $z = 4\text{\AA}$  between the substrate and the graphene layer and a Thomas-Fermi screening from the graphene electrons as described above [27]. As anticipated from the preceding discussion, the resistivity exhibits a characteristic exponential behavior. Note that unlike the short-range scattering from in-plane phonons, the present result has a sizable density dependence due to the long-range nature of the interaction. This is illustrated in Fig.2b, where we plot the dependence of  $\sigma$  on  $E_F$  at fixed  $T = 300, 200, 150\text{K}$  (from bottom to top). In the explored density range, the conductivity has an overall linear dependence on  $E_F$  away from the Dirac point, which is intermediate between the cases of short range scatterers ( $\sigma \sim \text{const}$ ) and charged impurities ( $\sigma \propto E_F^2$ )[15]. This behavior can be understood from standard dimensional arguments, observing that the scattering rate of Eq.(2) scales as  $M_{q \simeq k_F}^2 \propto k_F^{-1}$  times the density of states  $\propto k_F$ , which yields  $\Gamma \sim \text{const}$ . The result  $\sigma \propto |E_F|$  then follows directly from Eq. (3).

Superimposed to the smooth density dependence analyzed above, a slight “kink” appears in the electrical characteristic at  $E_F \simeq \omega_{s1}$  that testifies the interaction with the sharp interface phonon mode. The anomaly becomes more pronounced at low temperatures owing to the sharp Fermi function in the Kubo formula. There, however, the absolute value of the scattering rate becomes

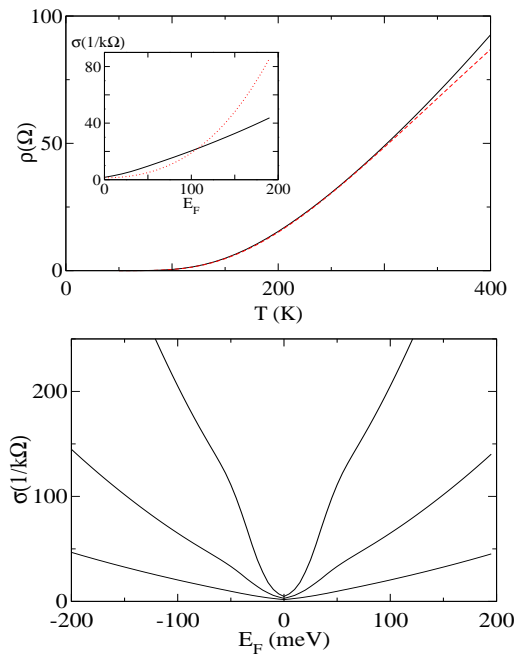


FIG. 2: a) Temperature dependence of the resistivity for  $E_F = 100\text{meV}$  (the dashed line corresponds to  $\rho = \rho_0 e^{-\omega_{s1}/T}$  with  $\rho_0 = 500\Omega$ ). b) Conductivity vs. chemical potential for  $T = 150, 200$  and  $300\text{K}$  (from top to bottom). The inset of a) shows the comparison with bilayer graphene (dotted line) at  $T = 300\text{K}$ .

extremely small, and it is likely to be completely hidden by the presence of other sources of scattering.

In the inset of Fig. 2b we compare the conductivity for single-layer and bilayer graphene at  $T = 300\text{K}$ . The different density of states in bilayer graphene leads to a stronger energy dependence. Accordingly, bilayer graphene should be a better conductor at large bias. With the present choice of parameters, the crossing occurs at  $E_F \sim 0.1\text{eV}$ .

*Finite distance cutoff.* The simple scaling argument presented above, leading to a linear dependence  $\sigma \propto |E_F|$  for single layer graphene, breaks down when  $2k_F z \sim 1$ . At larger densities, the short range cut-off associated to the distance  $z$  between the carriers and the interface must be taken into account explicitly. As a result, extra powers of  $k_F z$  arise in the scattering rate, due to the suppression of the angular factors  $[1 \pm \cos(\phi_{\mathbf{p}+\mathbf{q}} - \phi_{\mathbf{p}})]$  at large scattering angles, as well as the reduced available density of states. All together, these factors eventually lead to a  $\sigma \propto E_F^4$  dependence ( $\Gamma \propto |E_F|^3$ ). In Fig.3 we show plots of  $\sigma$  vs  $E_F$  at  $T = 300\text{K}$  for increasing values of  $z$ . While for  $z = 4\text{\AA}$  the behavior is approximately linear in the whole energy range, a clear upturn becomes visible at larger separations, reflecting the expected crossover at  $|E_F|z/v_F \sim 1/2$ . Notably, this phenomenon can lead to an apparent behavior  $\sigma \propto E_F^2 \propto n$  [13], which is best seen in the inset of Fig.3.

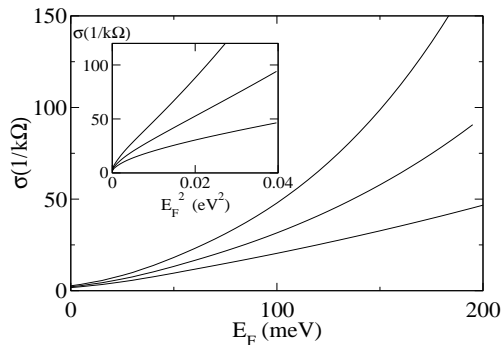


FIG. 3: Same as Fig 2.b, for different values of the distance  $z$ . From bottom to top,  $z = 4, 12$  and  $20$  Å. A crossover to a super-linear behavior is apparent at large  $z$  and large  $E_F$ . In the inset, the same data are plotted as a function of  $E_F^2 \propto n$ .

*Discussion.* Although the transport properties of graphene are roughly temperature independent below  $T = 100$ K, a sharp increase of the resistivity of the order of  $\Delta\rho \sim 100\Omega$  around room temperature has been reported in field-effect doped samples at  $n \gtrsim 10^{12}\text{cm}^{-2}$  [9, 10, 11, 12, 13]. This increase is unlikely to be due to the effects of disorder, which are expected to depend smoothly, if at all, on the temperature. As was mentioned above, also the in-plane optical phonons of graphene can be ruled out due to their high oscillation frequencies. That in-plane scattering is not the main cause of the observed behavior is further supported by the observation that the temperature dependent contribution to the resistivity is not independent of density [11, 13], pointing to a long-range scattering mechanism such as the one studied here. According to the present results, a density and temperature dependent contribution to the resistivity is compatible with the mechanism of remote phonon scattering.

*Conclusions.* We have estimated the quasiparticle scattering rates induced by the polar modes of  $\text{SiO}_2$  and  $\text{SiC}$  substrates on graphene. Our results show that, while remote phonon scattering has negligible effects on transport at low temperatures, it becomes relevant at room temperature, where it could constitute the dominant limiting factor of the electron mobility in sufficiently clean samples, especially for  $\text{SiO}_2$  substrates. According to the present scenario, the maximum conductivity that can be achieved in a given sample depends crucially on the dielectric properties of the gate insulator, so that the use of non-polar substrates should be favored to optimize the transport properties of graphene. We also find that the effects are reduced in doped bilayer graphene, which makes it more suitable for device applications at room temperature. On the opposite, larger effects can be expected when more polarizable substrates are used as gate dielectrics.

*Acknowledgements.* This work was supported by MEC (Spain) through grant FIS2005-05478-C02-01, the

Comunidad de Madrid, through the program CITEC-NOMIK, CM2006-S-0505-ESP-0337, and the European Union Contract 12881 (NEST). The authors thank M.S. Fuhrer for stimulating correspondence and T. Stauber for useful discussions.

- 
- [1] S. Q. Wang and G. D. Mahan, **6**, 4517 (1972).
  - [2] K. Hess and P. Vogl, Sol. State Commun. **30**, 807 (1979).
  - [3] M. V. Fischetti, D. A. Neumayer, and E. A. Cartier, Journ. Appl. Phys. **90**, 4587 (2001).
  - [4] R. Chau, S. Datta, M. Doczy, B. Doyle, J. Kavalieros, and M. Metz, IEEE Electron Device Letters **25**, 408 (2004).
  - [5] A. F. Stassen, R. W. I. de Boer, N. N. Iosad, and A. F. Morpurgo, Appl. Phys. Lett. **85**, 3899 (2004).
  - [6] I. N. Hulea, S. Fratini, H. Xie, C. L. Mulder, N. N. Iosad, G. Rastelli, S. Ciuchi, and A. F. Morpurgo, Nature Materials **5**, 982 (2006).
  - [7] A. K. Geim and K. S. Novoselov, Nature Materials **6**, 183 (2007).
  - [8] A. H. Castro Neto, F. Guinea, N. M. R. Peres, K. S. Novoselov, and A. K. Geim (2007), arXiv:0709.1163.
  - [9] E. W. Hill, A. K. Geim, K. S. Novoselov, F. Schedin, and P. Blake, IEEE Trans. Magn. **42**, 2694 (2006).
  - [10] Y.-W. Tan, Y. Zhang, H. L. Störmer, and P. Kim, Eur. Phys. J., Special Topics **148**, 15 (2007).
  - [11] S. V. Morozov, K. S. Novoselov, M. I. Katsnelson, F. Schedin, D. Elias, J. A. Jaszczak, and A. K. Geim (2007), arXiv:0710.5304.
  - [12] Y.-W. Tan, Y. Zhang, K. Bolotin, Y. Zhao, S. Adam, E. Hwang, S. Das Sarma, H. L. Störmer, and P. Kim, Phys. Rev. Lett., in press (2007).
  - [13] J. H. Chen, C. Jang, S. Xiao, M. Ishigami, M. S. Fuhrer, (2007) arXiv:0711.3646.
  - [14] K. S. Novoselov, D. Jiang, F. Schedin, T. J. Booth, V. V. Khotkevich, S. V. Morozov, and A. K. Geim, Proc. Nat. Acad. Sc. **102**, 10451 (2005).
  - [15] K. Nomura and A. H. MacDonald, Phys. Rev. Lett. **98**, 076602 (2007).
  - [16] S. Adam, E. H. Hwang, V. M. Galitski, and S. Das Sarma (2007), arXiv:0705.1540.
  - [17] K. Ziegler, Phys. Rev. B **75**, 233407 (2007).
  - [18] T. Stauber, N. M. R. Peres, and F. Guinea, Phys. Rev. B **76**, 205423 (2007).
  - [19] M. I. Katsnelson and A. K. Geim (2007), arXiv:0706.2490.
  - [20] E. H. Hwang and S. Das Sarma (2007), arXiv:0711.0754.
  - [21] N. Mori and T. Ando, Phys. Rev. B **40**, 6175 (1989).
  - [22] H. Nienhaus, T. U. Kampen, and W. Mönch, Surf. Sci. Letters **324**, L328 (1989).
  - [23] B. Özyilmaz, P. Jarillo-Herrero, D. Efetov, and P. Kim (2007), arXiv:0709.1731.
  - [24] B. Wunsch, T. Stauber, F. Sols, and F. Guinea, New J. Phys. **8**, 318 (2006).
  - [25] F. Guinea, Journ. Phys. C: Condens. Matt. **14**, 3345 (1981).
  - [26] G. D. Mahan, *Many Particle Physics* (Plenum Press, 2nd edition, 1990).
  - [27] This approximation assumes that the electrons respond instantaneously to the lattice vibrations, and therefore

constitutes a lower bound to the scattering rate. An upper bound is obtained by plainly neglecting screening which in the regime of interest here leads to resistivities

$\approx 4$  times larger than the ones shown.